Glycoconjugate Journal (2020) 37:119–128
https://doi.org/10.1007/s10719-019-09900-3

ORIGINAL ARTICLE

Interactions between Sclerostin and Glycosaminoglycans

Fuming Zhang [1] · Jing Zhao [2] · Xinyue Liu [2] · Robert J. Linhardt [1,2,3]

Received: 30 July 2019 / Revised: 20 November 2019 / Accepted: 26 November 2019 / Published online: 11 December 2019

Abstract

Sclerostin (SOST) is a glycoprotein having many important functions in the regulation of bone formation as a key negative regulator of Wnt signaling in bone. Surface plasmon resonance (SPR), which allows for a direct quantitative analysis of the label-free molecular interactions in real-time, has been widely used for the biophysical characterization of glycosaminoglycan (GAG)-protein interactions. In the present study, we report kinetics, structural analysis and the effects of physiological conditions (e.g., salt concentrations, Ca^{2+} and Zn^{2+}concentrations) on the interactions between GAGs and recombinant human (rh) and recombinant mouse (rm) SOST using SPR. SPR results revealed that both SOSTs bind heparin with high affinity (rhSOST-heparin, K_D~36 nM and rmSOST-heparin, K_D~77 nM) and the shortest oligosaccharide of heparin that effectively competes with full size heparin for SOST binding is octadecasaccharide (18mer). This heparin binding protein also interacts with other highly sulfated GAGs including, disulfated-dermatan sulfate and chondroitin sulfate E. In addition, liquid chromatography-mass spectrometry was used to characterize the structure of sulfated GAGs that bound to SOST.

Keywords Surface plasmon resonance · Sclerostin · Glycosaminoglycans · Heparin · Interaction

Introduction

Secreted from bone dwelling osteocytes, sclerostin (SOST) is a glycoprotein, which has important functions in the regulation of bone formation as a key negative regulator of Wnt signaling in bone [1, 2]. SOST reportedly interacts with a number of proteins including bone morphogenetic proteins (BMPs) -2, -4, -5, -6, -7 and low-density lipoprotein receptor-related protein (LRP) -5 and -6 [3–5], which are co-receptors in Wnt signaling system. These SOST involved interactions provide the important mechanisms of bone growth and remodeling through the modulation of Wnt/β-catenin signaling [6]. SOST has attracted considerable interest as a target for therapeutics to treat bone diseases, such as osteoporosis and sclerosteosis [1, 2]. SOST-specific antibodies have been developed and applied in animal studies resulting in significant increases in bone formation, bone density and bone strength [7] and a similar results were also reported in a human clinical trial by administration of a SOST neutralizing antibody showing a dose-dependent increase in markers of bone formation [8]. Romosozumab, a monoclonal anti-SOST antibody, has been used in the treatment of women with a high risk of osteoporotic fracture [9] and it was recently approved as a new drug from FDA in April 2019. SOST has also attracted researchers in the field of dentistry for the development of regenerative strategies with sclerostin as a target [10, 11].

Proteoglycans (PGs) are a family of biomacromolecules with a core protein to which one or more glycosaminoglycan (GAG) chains are covalently attached. Human bone cells produce a number of different PGs including, a large versican-like PG, a heparan sulfate syndecan-like PG, as well as biglycan (BGN) PG and decorin (DCN) PG [12, 13]. GAGs are usually classified into four disctint groups: heparin/heparan sulfate (HS), chondroitin sulfate/dermatan sulfate, keratan sulfate and hyaluronic acid based on their disaccharide backbones (Fig. 1). GAGs are key components of the bone

✉ Fuming Zhang
zhangf2@rpi.edu

✉ Robert J. Linhardt
linhar@rpi.edu

[1] Department of Chemical and Biological Engineering, Rensselaer Polytechnic Institute, Troy, NY 12180, USA

[2] Department of Chemistry and Chemical Biology, Center for Biotechnology and Interdisciplinary Studies, Rensselaer Polytechnic Institute, Troy, NY 12180, USA

[3] Departments of Biological Sciences and Biomedical Engineering, Center for Biotechnology and Interdisciplinary Studies, Rensselaer Polytechnic Institute, Troy, NY 12180, USA

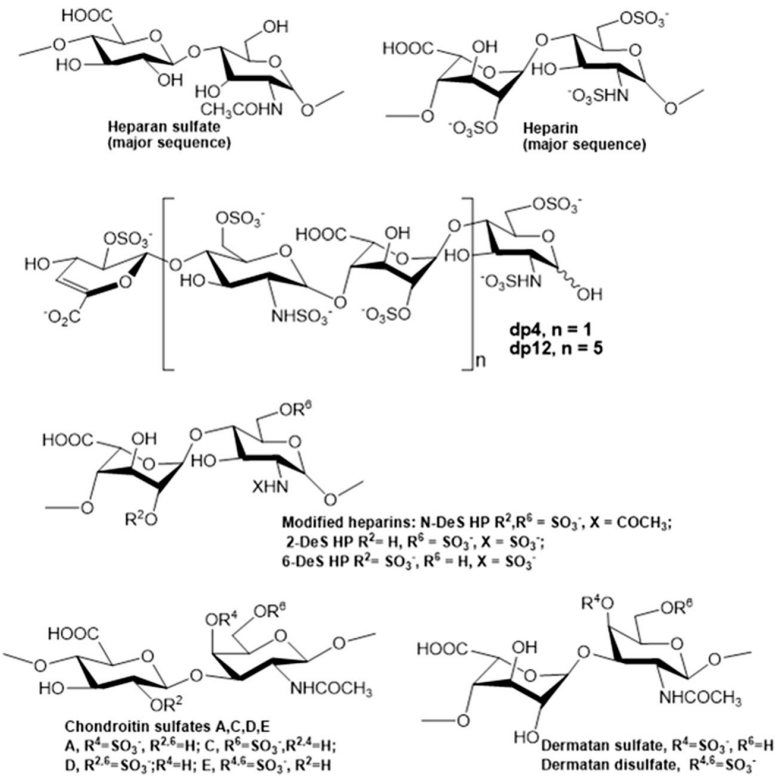

Fig. 1 Chemical structures of heparin, heparin-derived oligosaccharides and GAGs

matrix and cell surface that modulate the bioavailability and activity of various osteoclastic and osteogenic factors and play crucial biochemical and mechanical roles. For example, GAGs regulate the tissue-level hydration of bone, which affects the tissue-level toughness of bone (14). The reduction of GAGs in bone matrix is reportedly one of the molecular origins for age-related deterioration of bone quality [14]. HS has been shown to play key roles in the regulation of several important signaling pathways through the localization of proteins to specific cell surfaces and by direct association in the ligand-receptor interaction. The interaction between HS and SOST reportedly results in a significantly higher concentration of the protein at the surface of responsive cells [1]. Mansouri *et al*. [15] reported that osteoblastic HS controls bone remodeling by regulating Wnt signaling and the crosstalk between bone surface and marrow cells. In mucopolysaccharidosis type I, GAG accumulation and altered interactions with growth factors are the main causes for bone disease [16]. Chemically sulfated hyaluronic acid has been shown to bind sclerostin and improve bone regeneration of diabetic rats [17]. While these reports have provided a general functional understanding of GAG-SOST interactions, there is a lack of structural (i.e., GAG degree of sulfation and chain length) and biophysical data on these interactions.

In this study, the kinetics of the interaction between SOST and heparin (as a model GAG) was studied using a Biacore SPR system. Competition studies between the heparin on the chip surface and different GAGs in the solution phase were conducted to determine the binding preferences of SOST to GAGs. Similarly, competition studies with heparin-derived oligosaccharides having different chain sizes and with different chemically modified heparins were conducted to determine the chain-size dependence and the effect of different sulfo groups on sclerostin-heparin interactions. The effects of salt concentrations and various salt species (Ca^{2+} and Zn^{2+}) on these interactions were also investigated. In addition, liquid chromatography-mass spectrometry (LC-MS) was used to characterize the structure of sulfated glycans that bound to SOST. A detailed understanding of SOST and heparin/GAG interaction at the molecular level is of fundamental importance in the development of novel biomaterials for bone diseases.

Materials and methods

Materials

Recombinant human sclerostin (rhSOST) and mouse sclerostin (rmSOST) were purchased from R&D Systems (Minneapolis, MN). The GAGs used in this study were porcine intestinal heparin (average molecular weight, MW_{avg} = 16 kDa) and porcine intestinal heparan sulfate (HS) (MW_{avg} = 14 kDa) from Celsus Laboratories (Cincinnati, OH); chondroitin sulfate A (CSA, MW_{avg} = 20 kDa) from porcine rib

cartilage (Sigma, St. Louis, MO), chondroitin sulfate B (CSB)/dermatan sulfate (DS, MW_{avg} = 30 kDa) from porcine intestine (Sigma), chondroitin sulfate C (CSC, MW_{avg} = 20 kDa) from shark cartilage (Sigma), chondroitin sulfate D (CSD, MW_{avg} = 20 kDa) from whale cartilage (Seikagaku, Tokyo, Japan) and chondroitin sulfate E (CSE, MW_{avg} = 20 kDa) from squid cartilage (Seikagaku). Low molecular weight heparin (LMWH, MW_{avg} = ~6.5 kDa) and dermatan disulfate (Dis-DS, MW_{avg} = 33 kDa) were from Celsus Laboratories (Cincinnati, OH). *N*-desulfated, *N*-acetylated heparin (*N*-DeS HP, MW_{avg} = 14 kDa) and 2-*O*-desulfated heparin (2-DeS HP, MW_{avg} = 13 kDa) were all prepared based on Yates *et al.* [18]. A 6-*O*-desulfated heparin derivative (6-DeS HP, MW_{avg} = 13 kDa) was provided by Professor Lianchun Wang (University of South Florida). Polyacrylamide gel electrophoresis (PAGE) was applied to determine the MW_{avg} of each GAG using a standard composed of a mixture of oligosaccharides of known molecular weight followed a protocol developed in our lab [19]. Heparin oligosaccharides included tetrasaccharide (degree of polymerization (dp)4), hexasaccharide (dp6), octasaccharide (dp8), decasaccharide (dp10), dodecasaccharide (dp12), tetradecasaccharide (dp14), hexadecasaccharide (dp16) and octadecasaccharide (dp18) and were prepared from porcine intestinal heparin by controlled partial heparin lyase I treatment and followed by size fractionation. The chemical structures of these GAGs are shown in Fig. 1. Sensor SA chips were from GE Healthcare (Uppsala, Sweden). SPR measurements were performed on a BIAcore 3000 operated using BIAcore 3000 control and the sensorgarms were processed using BIAevaluation software (version 4.0.1). Unsaturated heparin/HS disaccharide standards (0S: ΔUA–GlcNAc; NS: ΔUA–GlcNS; 6S: ΔUA–GlcNAc6S; 2S: ΔUA2S–GlcNAc; NS2S: ΔUA2S–GlcNS; NS6S: ΔUA–GlcNS6S; 2S6S: ΔUA2S–GlcNAc6S; TriS: ΔUA2S–GlcNS6S) were purchased from Iduron (Manchester, UK). Tributylamine was purchased from Sigma. Ammonium acetate, acetic acid, water and acetonitrile were of HPLC grade (Fisher Scientific, Springfield, NJ). Microcon Centrifugal Filter Units YM-10 was obtained from Millipore (Bedford, MA, USA). *Escherichia coli* expression and purification of the recombinant *Flavobacterium heparinum* heparin lyase I, II, III (Enzyme Commission (EC) #s 4.2.2.7, 4.2.2.X, 4.2.2.8) were prepared in our laboratory as previously described [20].

Preparation of heparin biochip

The preparation of biotinylated heparin was followed our previous protocol [21]. In brief, 200 μL of water, 2 mg of heparin and 2 mg of amine–PEG_3–Biotin (Thermo Scientific, Waltham, MA) were mixed with 10 mg of $NaCNBH_3$. The initial reaction was carried at 70 °C for 24 h, and then a further 10 mg of $NaCNBH_3$ was added to continue running the reaction for another 24 h. After complete the reaction, the mixture was desalted with a spin column (3000 molecular weight cut-off) and was freeze-dried for chip preparation. The biotinylated heparin was immobilized to a streptavidin (SA) chip based on the manufacturer's protocol. In brief, 20 μL solution of the heparin-biotin conjugate (0.1 mg/mL) in HBS-EP running buffer was injected over flow cell 2 (FC2) of the SA chip at a flow rate of 10 μL/min. The successful immobilization of heparin was confirmed by the observation of a ~200 resonance unit (RU) increase in the sensor chip. The control flow cell (FC1) was prepared by 1 min injection with saturated biotin.

Kinetic measurement of interaction between heparin and SOST

Both rhSOST or rmSOST samples were diluted in HBS-EP buffer (0.01 M HEPES, 0.15 M NaCl, 3 mM EDTA, 0.005% surfactant P20, pH 7.4). Different dilutions of these two protein samples were injected at a flow rate of 30 μL/min. At the end of the sample injection, HBS-EP buffer was flowed over the sensor surface to facilitate dissociation. After a 3 min dissociation time, the sensor surface was regenerated by injecting with 30 μL of 0.5% SDS, then with 30 μL of 2 M NaCl to obtain a fully regenerated surface. The response was monitored as a function of time (sensorgram) at 25 °C.

Solution competition study between heparin on chip surface and heparin-derived oligosaccharides in solution using SPR

Both rhSOST and rmSOST (2.5 nM) were individually mixed with 100 nM of heparin oligosaccharides, including tetrasaccharide (dp4), hexasaccharide (dp6), octasaccharide (dp8), decasaccharide (dp10), dodecasaccharide (dp12), tetradecasaccharide (dp14), hexadecasaccharide (dp16) and octadecasaccharide (dp18) in HBS-EP buffer, and were injected over the heparin chip each at a flow rate of 30 μL/min. After each run, the dissociation and the regeneration steps were performed as described above. For each set of competition experiments on SPR, a control experiment (only protein without any heparin or oligosaccharides) was performed to make sure the surface was completely regenerated and that the results obtained between runs were comparable.

Solution competition study between heparin on the chip surface and GAGs, chemically modified heparin in solution using SPR

For the testing of inhibition of other GAGs and chemically modified heparins to the SOST-heparin interaction, rhSOST or rmSOST at a concentration of 5 nM was pre-mixed with 100 nM of GAG or chemically modified heparin and injected

over the heparin chip at a flow-rate of 30 μL/min. After each run, a dissociation period and regeneration protocol was performed as previously described.

Measurement of the effects of physiological conditions on the interaction between heparin and SOST using SPR

Both rhSOST and rmSOST were individully diluted in HBS-P buffer (0.01 M HEPES, 0.15 M NaCl, 0.005% surfactant P20, pH 7.4). The rhSOST or rmSOST samples in buffers having different physiological components (i.e., Na^+ concentration, Ca^{2+} and Zn^{2+} concentration) were injected at a flow rate of 30 μL/min.

Filter trapping of HS dp10 binding to SOST and composition analysis using LC – MS.

HS dp10 was prepared from porcine intestinal HS with partial heparin lyase III degradation and followed by size fractionation with P10 column. The protocol of filter trapping of HS dp10 with protein was followed our previous report [22]. In brief, HS dp10 was mixed with SOST in buffer with 25 mM Hepes and 150 mM NaCl (pH 7.4) and incubated at room temperature for 1 h. The nonbinding oligosaccharides were removed from the mixture using spin columns (MWCO of 10 kDa), which were washed three times with buffer. The high-affinity oligosaccharides were subjected to disaccharide compositional analysis using LC − MS [22].

Statistical analysis

Data are expressed as mean ± standard error (SE). Statistical analysis was performed using Student's t test in Prism 8 (GraphPad, San Diego, USA). All results (labeled *$p < 0.05$, **$p < 0.001$) were considered statistically significant at *p < 0.05 versus control.

Results and discussion

Kinetic measurements of SOST-heparin interactions

Previous report showed that SOST is a heparin-binding protein (HBP) [1]. In the current study, we utilized SPR system to measure the binding kinetics and affinity of SOST-heparin interaction using a sensor chip with immobilized heparin. Sensorgrams of SOST-heparin interaction are shown in Fig. 2. The sensorgrams were fit globally to obtain association rate constant (*ka*), dissociation rate constant (*kd*) and equilibrium dissociation constant (K_D) (Table 1) using the BiaEvaluation software and assuming a 1:1 Langmuir model. SPR analysis demonstrated that rhSOST and rmSOST bound

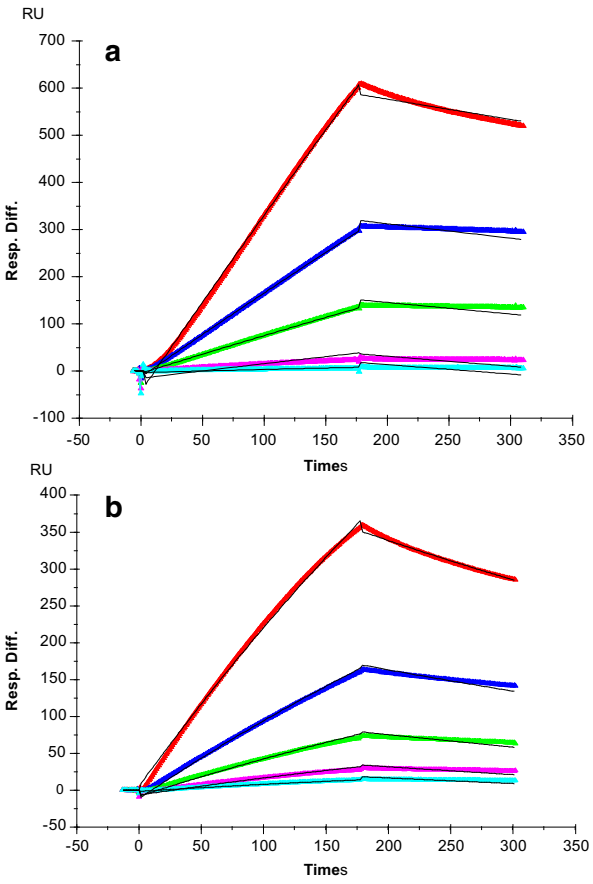

Fig. 2 **A:** SPR sensorgrams of rhSOST-heparin interaction. **B:** SPR sensorgrams of rmSOST-heparin interaction. Concentrations of rhSOST or rmSOST (from top to bottom): 5, 2.5, 1.25, 0.63 and 0.32 nM, respectively. The black curves are the fitting curves using 1:1 Langmuir binding model from BIAevaluate 4.0.1

to heparin in nanomolar affinity (rhSOST- heparin, K_D~36 nM and rmSOST-heparin, K_D~77 nM). The small difference of binding kinetics between rhSOST-heparin and rmSOST-heparin could be due the difference in protein sequence. Based on the amino acid alignment analysis using the Basic Local Alignment Search Tool (BLAST), rhSOST and rmSOST share 87.3% of similarity.

Table 1 Summary of kinetic data of sclerostin-heparin interactions*

Interaction	k_a *(1/MS)*	k_d *(1/S)*	K_D *(M)*
rhSOST/Heparin	1.04×10^4 (± 461)	3.77×10^{-4} ($\pm 1.59 \times 10^{-5}$)	3.62×10^{-8}
rmSOST/Heparin	1.90×10^4 (± 819)	1.46×10^{-3} ($\pm 2.01 \times 10^{-5}$)	7.68×10^{-8}

*The data with (±) in parentheses are the standard deviations (SD) from global fitting of five injections

Solution competition study on the interaction between surface-bound heparin and SOST to heparin-derived oligosaccharides in solution using SPR

Solution/surface competition experiments were performed by SPR to examine the effect of the saccharide chain size of heparin on the SOST-heparin interaction. Different size heparin-derived oligosaccharides (from dp4 to dp18) were used in the competition study. The same concentration (100 nM) of heparin oligosaccharides were mixed in the rhSOST (2.5 nM)/heparin interaction solution. Only small competition effect (<20%) was observed when 100 nM of oligosaccharides (from dp 4 to dp16), present in the protein solution. For the rest tested oligosaccharide (dp18), LMWH and full chain heparin, dramatically decreased rhSOST binding signal was observed (Fig. 3). The rmSOST showed a similar competition pattern as rhSOST in this solution competition analysis. The variation of the SOST binding showed in this competition experiment suggests that the interaction between SOST and heparin is chain-length dependent and SOST prefers to bind long chain heparin (≥dp18). It was reported that SOST molecule basically is linear, positively charged patch, which covers one entire side of the protein (1). Based on the computational model (1), the putative heparin binding site on SOST covers over surface of ~52 Å in length, which is comparable to the length expected for a 18-mer heparin molecule (72 Å). Most of heparin-protein interactions are chain-length dependent, for example, the formation of a ternary complex between AT, thrombin, and heparin requires at least 18 saccharide units for efficient formation [23], but AT-based antifactor Xa activity requires only the pentasaccharide-binding site.

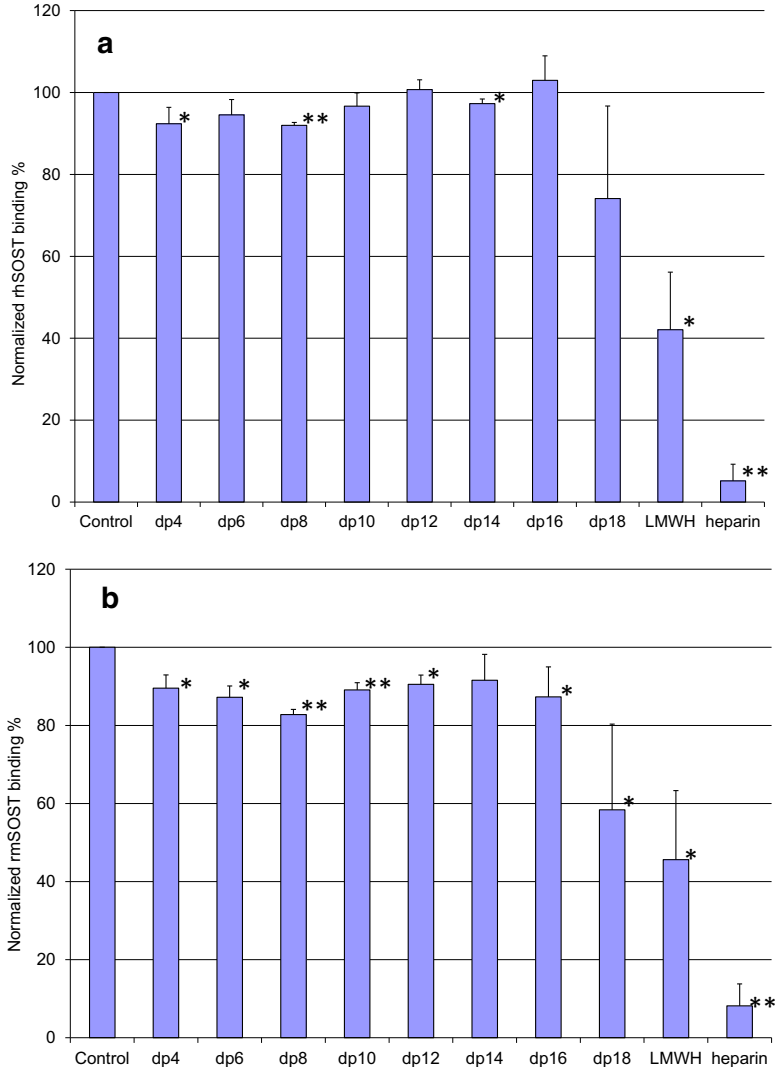

Fig. 3 Bar graphs (based on triplicate experiments with standard deviation) of normalized rhSOST or rmSOST binding preference to surface heparin by competing with different size of heparin oligosaccharides in solution. SOST concentration was 2.5 nM, and concentrations of heparin oligosaccharides in solution were 100 nM. **A**: rhSOST, **B:** rmSOST (*$p < 0.05$, **$p < 0.001$)

SPR solution competition study of different chemical modified heparins

SPR bar graphs of the chemical modified heparin competition levels are shown in Fig. 4. The results demonstrate that all the three chemical modified heparins (*N*-desulfated, *N*-acetylated heparin, 2-*O*-desulfated heparin and 6-*O*-desulfated heparin) giving reduced inhibitory activities. A much greater reduction in inhibitory activities was observed for *N*-desulfated, *N*-acetylated heparin than 6-*O*-desulfated heparin or 2-*O*-desulfated heparin suggesting that the 2-*O*-sulfo and 6-*O*-sulfo groups on heparin have less impact than the *N*-sulfo groups on the SOST-heparin interaction. Similar effects of sulfation pattern on heparin/HS protein interactions were observed in our previous studies, including studies on the interactions of langerlin-heparin, Robo1-heparin, TIMP3-heparin [22, 24, 25].

SPR solution competition study of different GAGs

The SPR competition assay was also utilized to determine the binding preference of SOST to various GAGs (Fig. 1). SPR competition bar graphs of the GAG competition levels are shown in Figs. 5. For both rhSOST and rmSOST, CSE and DiS-DS produced inhibition by competing 50–60% of the SOST binding to immobilized heparin on the chip surface. Weak or no inhibitory activities were observed for HS, CS-A, DS, CS-C and CS-D. These data suggest that the binding interactions of SOST to GAGs appear structure-dependent and highly influenced by the level of GAG sulfation since heparin, CSE and DiS-DS have a higher level of sulfation than the other GAGs tested.

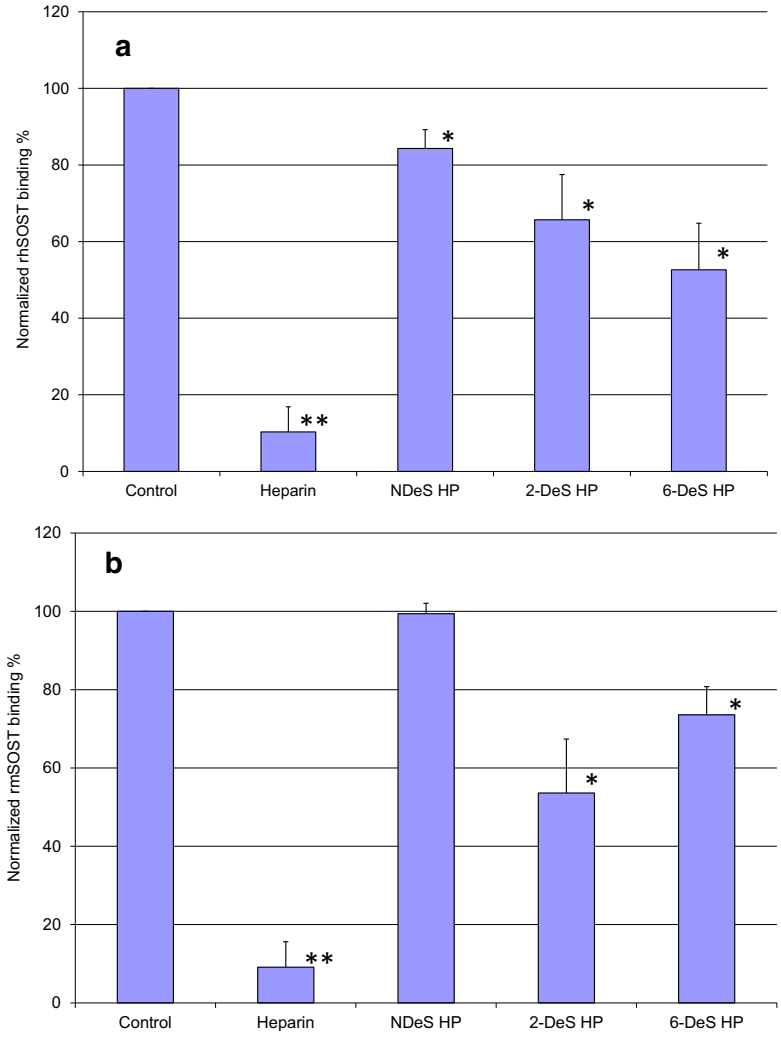

Fig. 4 Bar graphs (based on triplicate experiments with standard deviation) of normalized rhSOST or rmSOST binding preference to surface heparin by competing with different chemical modified heparins in solution. SOST concentration was 2.5 nM, and concentrations of chemical modified heparins in solution were 100 nM. **A**: rhSOST, **B:** rmSOST (*$p < 0.05$, **$p < 0.001$)

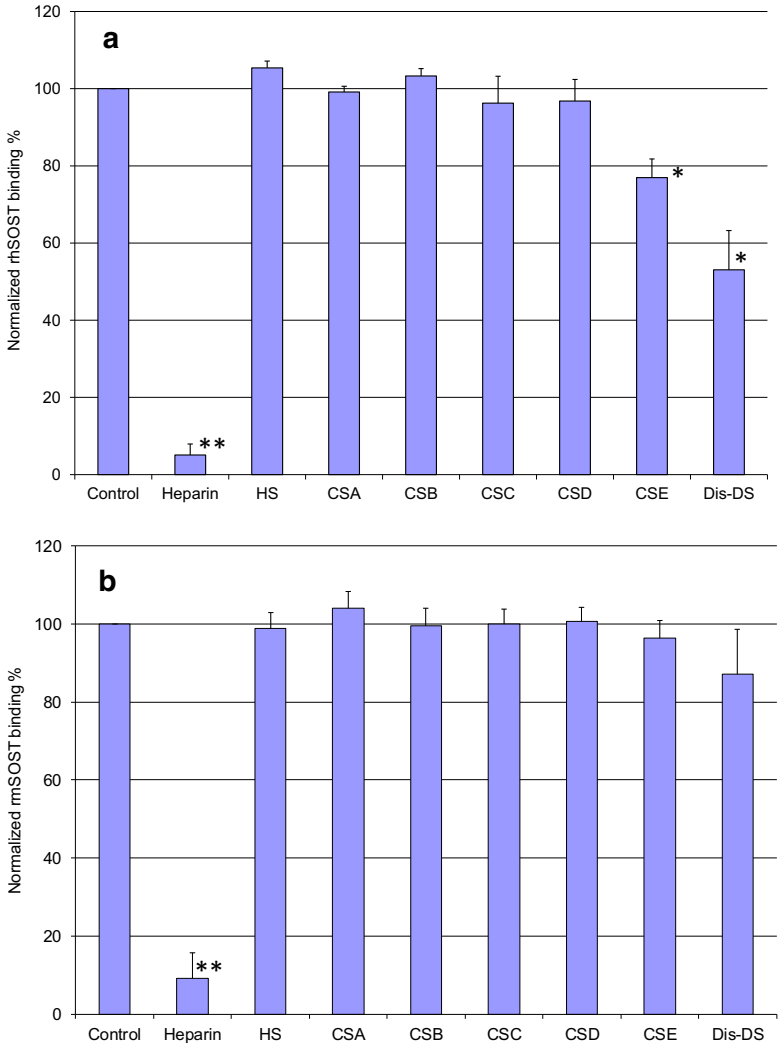

Fig. 5 Bar graphs (based on triplicate experiments with standard deviation) of normalized rhSOST or rmSOST binding preference to surface heparin by competing with different GAGs in solution. Sclerostin concentration was 2.5 nM, and concentrations of GAGs in solution were 100 nM. **A**: rhSOST, **B:** rmSOST (*$p < 0.05$, **$p < 0.001$)

The effects of salt concentrations on the interaction between heparin and SOST

Binding buffers with different salt (NaCl) concentrations (150 mM, as control, 300 mM, 500 mM and 1000 mM NaCl) were used for the SPR analysis to assess the effect of salt conditions on SOST-heparin interaction. The results of SOST-heparin interaction in various NaCl concentration are shown in Fig. 6 A and B. The results reveal that SOST-heparin interaction is very sensitive to NaCl concentration and higher salt concentrations (0.3 M to 1 M NaCl) inhibit all binding to heparin. The data suggests that SOST-heparin interaction is primarily an electrostatically driven interaction.

The impact of Ca^{2+} and Zn^{2+} on SOST-heparin interaction was also assessed. The SPR measurements on SOST-heparin interaction were conducted through the addition of $CaCl_2$ or $ZnCl_2$ at concentration of 0, 10, 100 and 1000 μM, respectively. The results (Figs. 6C and D) showed the SOST binding to heparin was enhanced with addition of Ca^{2+} at 10 μM, 100 and 1000 μM concentrations of Ca^{2+} in different levels and the highest binding promotion to heparin for rhSOST and rmSOST was observed at 10 μM and 1000 μM of Ca^{2+} added. The impact of Zn^{2+} on SOST-heparin interaction showed a similar pattern to Ca^{2+}, except SOST binding was reduced on addition of 1000 μM Zn^{2+}. The enhancement of SOST binding to heparin with the addition of Ca^{2+}/Zn^{2+} suggests that SOST may be able to coordinate calcium impacting heparin binding, similar to the coordination found for the annexin A2-heparin interaction [26]. Previous reports showed that some divalent metal ions (e.g., Ca^{2+}, Zn^{2+} and Cu^{2+}) are necessary in many protein-heparin interactions, which affect the binding affinity, specificity and stability of these complexes [27–29].

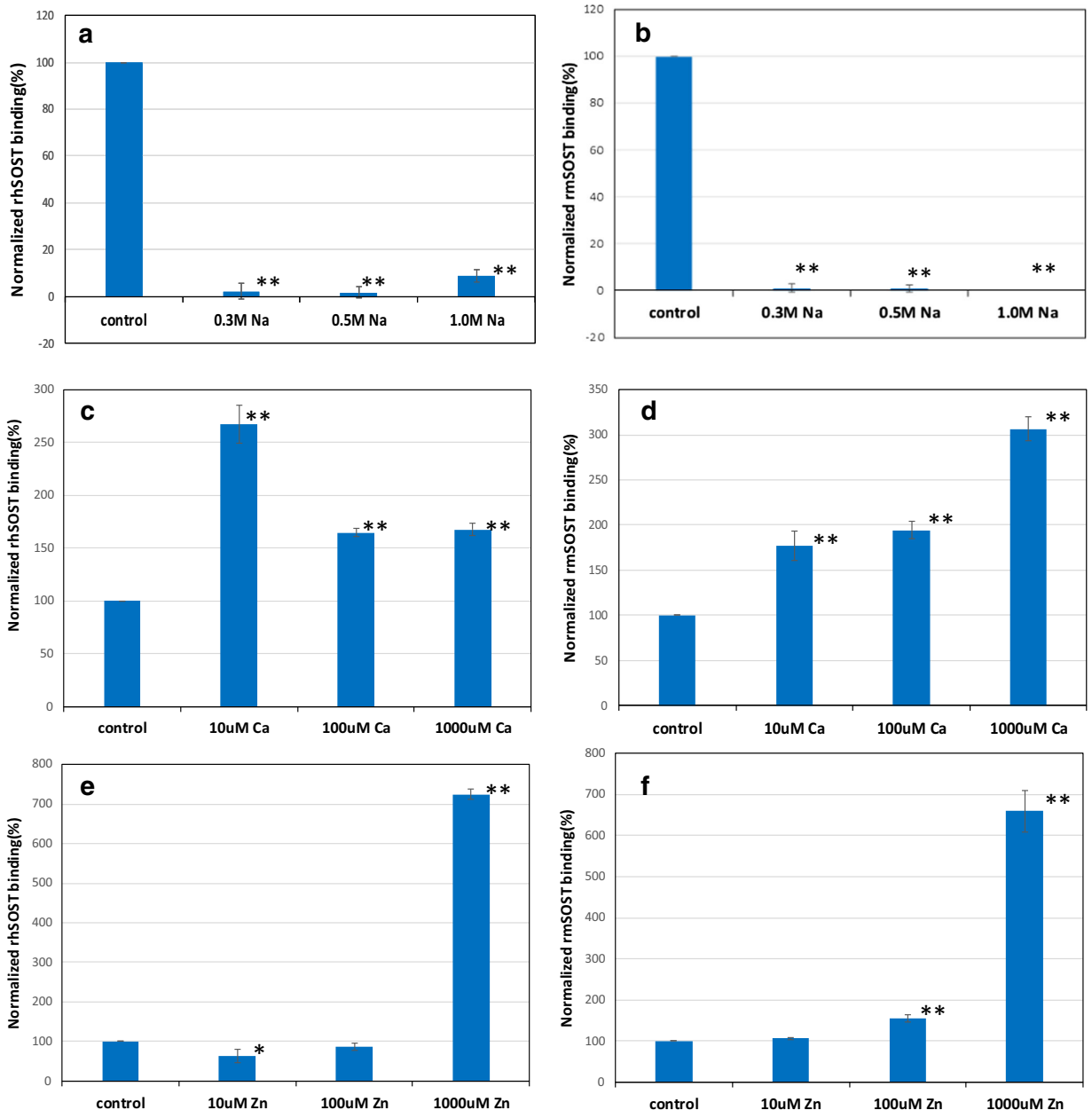

Fig. 6 SPR analysis of the effects of salt concentrations on the interactions between heparin and SOST. The effect of salt (NaCl) concentration on the heparin-SOST interaction: **A**: rhSOST, **B:** rmSOST; The effect of Ca^{2+} on heparin-SOST interaction with the addition of $CaCl_2$ (0, 10, 100 and 1000 μM), **C**: rhSOST, **D:** rmSOST; The effect of Zn^{2+} on heparin-SOST interaction with the addition of $ZnCl_2$ (0, 10, 100 and 1000 μM), **C**: rhSOST, **D:** rmSOST (*p < 0.05, **p < 0.001)

Structural analysis on the specific oligosaccharides binding to SOST

A filter trapping experiment was conducted using SOST to catch the preferred sequence from HS-derived oligosaccharides to further investigate the fine structural specificity of heparin/HS for the SOST interaction. Our previous report showed HS dp10 oligosaccharide with diversity of the disaccharide compositional structures is a good candidate for filter trapping experiment [30]. The high-affinity oligosaccharides caught by SOST were then subjected to disaccharide compositional analysis using LC-MS. These results showed the HS dp10 that bound to both SOST was clearly enriched in NS and 6S disaccharide in comparison to the original HS dp10 but

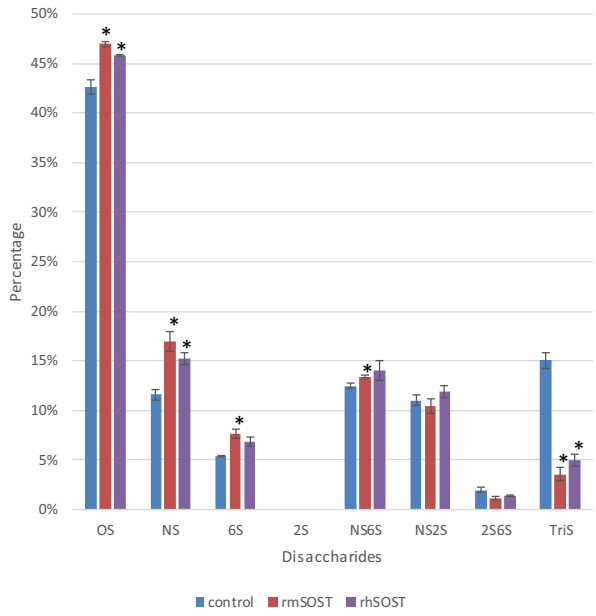

Fig. 7 Disaccharides compositional analysis of HS dp10 binding to rhSOST or rmSOST using LC-MS (*p < 0.05, **p < 0.001)

contained a surprisingly reduced amount of tri-S disaccharide. These results partially agree with the SPR data showing the *N*-sulfation on heparin is important for the SOST-heparin interaction but suggest that possibly simply having a high sulfation level was insufficient for tight binding (Fig. 7).

In conclusion, SPR analysis shows that SOST is a heparin-binding protein with high affinity, with heparin binding to rhSOST with a K_D~36 nM and to rmSOST with a K_D~77 nM. The SPR solution competition study demonstrates that SOST binding to heparin is chain length dependent and it prefers to bind full chain heparin or large oligosaccharides (dp18). Higher sulfation levels of GAGs generally enhance their binding affinities, i.e., CSE and Dis-DS showed high inhibitions to SOST-heparin interaction. *N*-sulfo and 6-*O*-sulfo groups on heparin are required for the SOST-heparin interaction. The interactions are greatly affected by the salt conditions NaCl concentrations, and in particular by divalent cations Ca^{2+}, and Zn^{2+}. The interaction studies and structural characterization conducted here should be useful for the development of GAG based regenerative biomaterials and for understanding the roles of SOST with it therapeutic applications.

Acknowledgements This work was supported by National Institutes of Health Grants: DK111958, CA231074 and AG062344 to R.J.L.

Compliance with ethical standards

Conflicts of interest The authors declare that they have no conflicts of interest.

Ethical approval This article does not contain any studies with human participants or animals performed by any of the authors.

Abbreviations *SOST,* Sclerostin; *GAG,* Glycosaminoglycan; *rhSOST,* Recombinant human sclerostin; *rmSOST,* Recombinant mouse sclerostin; *SPR,* Surface plasmon resonance; *HS,* Heparan sulfate; *CSA,* Chondroitin sulfate A; *CSB,* Chondroitin sulfate B; *DS,* Dermatan sulfate; *CSC,* Chondroitin sulfate C; *CSD,* Chondroitin sulfate D; *CSE,* Chondroitin sulfate E; *LMWH,* Low molecular weight heparin; *SA,* Streptavidin; *dp,* Degree of polymerization

References

1. Veverka, V., Henry, A.J., Slocombe, P.M., Ventom, A., Mulloy, B., Muskett, F.W., Muzylak, M., Greenslade, K., Moore, A., Zhang, L., Gong, J., Qian, X., Paszty, C., Taylor, R.J., Robinson, M.K., Carr, M.D.: Characterization of the structural features and interactions of sclerostin: molecular insight into a key regulator of Wnt-mediated bone formation. J. Biol. Chem. **84**, 10890–10900 (2009)
2. van Bezooijen, R.L., Roelen, B.A., Visser, A., van der Wee-Pals, L., de Wilt, E., Karperien, M., Hamersma, H., Papapoulos, S.E., ten Dijke, P., Löwik, C.W.: Sclerostin is an osteocyte-expressed negative regulator of bone formation, but not a classical BMP antagonist. J. Exp. Med. **199**, 805–814 (2004)
3. Winkler, D.G., Yu, C.P., Geoghegan, J.C., Ojala, E.W., Skonier, J.E., Shpektor, D., Sutherland, M.K., Latham, J.: A: Sclerostin inhibition of Wnt-3a-induced C3H10T1/2 cell differentiation is indirect and mediated by bone morphogenetic proteins. J. Biol. Chem. **279**, 36293–36298 (2004)
4. Kusu, N., Laurikkala, J., Imanishi, M., Usui, H., Konishi, M., Miyake, A., Thesleff, I., Itoh, N.: Sclerostin is a novel secreted osteoclast-derived bone morphogenetic protein antagonist with unique ligand specificity. J. Biol. Chem. **278**, 24113–24117 (2003)
5. Li, X.F., Zhang, Y.Z., Kang, H.S., Liu, W.Z., Liu, P., Zhang, J.G., Harris, S.E., Wu, D.Q.: Sclerostin binds to LRP5/6 and antagonizes canonical Wnt signaling. J. Biol. Chem. **280**, 19883–19887 (2005)
6. van Bezooijen, R.L., Svensson, J.P., Eefting, D., Visser, A., van der Horst, G., Karperien, M., Quax, P.H., Vrieling, H., Papapoulos, S.E., ten Dijke, P., Lowik, C.W.: Wnt but not BMP signaling is involved in the inhibitory action of sclerostin on BMP-stimulated bone formation. J. Bone Miner. Res. **22**, 19–28 (2007)
7. Ominsky, M.S., Vlasseros, F., Jolette, J., Smith, S.Y., Stouch, B., Doellgast, G., Gong, J., Gao, Y., Cao, J., Graham, K., Tipton, B., Cai, J., Deshpande, R., Zhou, L., Hale, M.D., Lightwood, D.J., Henry, A.J., Popplewell, A.G., Moore, A.R., Robinson, M.K., Lacey, D.L., Simonet, W.S., Paszty, C.: Two doses of sclerostin antibody in cynomolgus monkeys increases bone formation, bone mineral density, and bone strength. J. Bone. Miner. Res. **25**, 948–959 (2010)
8. Florio, M., Gunasekaran, K., Stolina, M., Li, X., Liu, L., Tipton, B., Salimi-Moosavi, H., Asuncion, F.J., Li, C., Sun, B., Tan, H.L., Zhang, L., Han, C.Y., Case, R., Duguay, A.N., Grisanti, M., Stevens, J., Pretorius, J.K., Pacheco, E., Jones, H., Chen, Q., Soriano, B.D., Wen, J., Heron, B., Jacobsen, F.W., Brisan, E., Richards, W.G., Ke, H.Z., Ominsky, M.S.: A bispecific antibody targeting sclerostin and DKK-1 promotes bone mass accrual and fracture repair. Nat. Commun. **7**, 11505
9. Saag, K.G., Petersen, J., Brandi, M.L., Karaplis, A.C., Lorentzon, M., Thomas, T., Maddox, J., Fan, M., Meisner, P.D., Grauer, A.: Romosozumab or alendronate for fracture prevention in women with osteoporosis. N. Engl. J. Med. **377**, 1417–1427 (2017)
10. Samiei, M., Janjić, K., Cvikl, B., Moritz, A., Agis, H.: The role of sclerostin and dickkopf-1 in oral tissues–A review from the

perspective of the dental disciplines. F1000Research. (2019). https://doi.org/10.12688/f1000research.1780
11. Taut, A.D., Jin, Q., Chung, J.H., Galindo-Moreno, P., Yi, E.S., Sugai, J.V., Ke, H.Z., Liu, M., Giannobile, W.V.: Sclerostin antibody stimulates bone regeneration after experimental periodontitis. J. Bone Miner. Res. **28**, 2347–2356 (2013)
12. Beresford, J.N., Fedarko, N.S., Fisher, L.W., Midura, R.J., Yanagishita, M., Termine, J.D., Robey, P.G.: Analysis of the proteoglycans synthesized by human bone cells *in vitro*. J. Biol. Chem. **262**, 17164–17172 (1987)
13. Salbach, J., Rachner, T.D., Rauner, M., Hempel, U., Anderegg, U., Franz, S., Simon, J.C., Hofbauer, L.C.: Regenerative potential of glycosaminoglycans for skin and bone. J. Mol. Med. **90**, 625–635 (2012)
14. Wang, X., Hua, R., Ahsan, A., Ni, Q., Huang, Y., Gu, S., Jiang, J.X.: Age-related deterioration of bone toughness is related to diminishing amount of matrix glycosaminoglycans (GAGs). JBMR Plus. **2**, 164–173 (2018)
15. Mansouri, R., Jouan, Y., Hay, E., Blin-Wakkach, C., Frain, M., Ostertag, A., Le Henaff, C., Marty, C., Geoffroy, V., Marie, P.J., Cohen-Solal, M., Modrowski, D.: Osteoblastic heparan sulfate glycosaminoglycans control bone remodeling by regulating Wnt signaling and the crosstalk between bone surface and marrow cells. Cell Death Dis. **8**, e2902 (2017)
16. Kingma, S.D.K., Wagemans, T., Ijlst, L., Bronckers, A.L.J.J., van Kuppevelt, T.H., Everts, V., Wijburg, F.A., van Vlies, N.: Altered interaction and distribution of glycosaminoglycans and growth factors in mucopolysaccharidosis type I bone disease. Bone. **88**, 92–100 (2016)
17. Picke, A.-K., Salbach-Hirsch, J., Hintze, V., Rother, S., Rauner, M., Kascholke, C., Möller, S., Bernhardt, R., Rammelt, S., Pisabarro, M.T., Ruiz-Gómez, G., Schnabelrauch, M., Schulz-Siegmund, M., Hacker, M.C., Scharnweber, D., Hofbauer, C., Hofbauer, L.C.: Sulfated hyaluronan improves bone regeneration of diabetic rats by binding sclerostin and enhancing osteoblast function. Biomaterials. **96**, 11–23 (2016)
18. Yates, E.A., Santini, F., Guerrini, M., Naggi, A., Torri, G., Casu, B.: ^{1}H and ^{13}C NMR spectral assignments of the major sequences of twelve systematically modified heparin derivatives. Carbohydr. Res. **294**, 15–27 (1996)
19. Edens, R.E., Al-Hakim, A., Weiler, J.M., Rethwisch, D.G., Fareed, J., Linhardt, R.J.: Gradient polyacrylamide gel electrophoresis for determination of the molecular weights of heparin preparations and low-molecular-weight heparin derivatives. J. Pharm. Sci. **81**, 823–827 (1992)
20. Linhardt, R.J., Turnbull, J.E., Wang, H.M., Loganathan, D., Gallagher, J.T.: Examination of the substrate specificity of heparin and heparan sulfate lyases. Biochemistry. **29**, 2611–2617 (1990)
21. Kim, S.Y., Zhao, J., Liu, X., Fraser, K., Lin, L., Zhang, F., Dordick, J.S., Linhardt, R.J.: Interaction of Zika virus with Glycosaminoglycans. Biochemistry. **56**, 1151–1162 (2017)
22. Zhao, J., Liu, X., Kao, C., Zhang, E., Li, Q., Zhang, F., Linhardt, R.J.: Kinetic and structural studies of interactions between glycosaminoglycans and langerin. Biochemistry. **55**, 4552–4559 (2016)
23. Petitou, M., Hérault, J.P., Bernat, A., Driguez, P.A., Duchaussoy, P., Lormeau, J.C., Herbert, J.M.: Synthesis of thrombin-inhibiting heparin mimetics without side effects. Nature. **398**, 417–422 (1999)
24. Zhang, F., Moniz, H.A., Walcott, B., Moremen, K.W., Linhardt, R.J., Wang, L.: Characterization of the interaction between Robo1 and heparin and other glycosaminoglycans. Biochimie. **95**, 2345–2353 (2013)
25. Zhang, F., Lee, K.B., Linhardt, R.J.: SPR biosensor probing the interactions between TIMP-3 and heparin/GAGs. Biosensors. **5**, 500–512 (2015)
26. Shao, C., Zhang, F., Kemp, M.M., Linhardt, R.J., Waisman, D.M., Head, J.F., Seaton, B.A.: Crystallographic analysis of calcium-dependent heparin binding to annexin A2. J. Biol. Chem. **281**, 31689–31695 (2006)
27. Lages, B., Stivala, S.S.: Interaction of polyelectrolyte heparin with copper(II) and calcium. Biopolymers. **12**, 127–143 (1973)
28. Chevalier, F., Lucas, R., Angulo, J., Martin-Lomas, M., Nieto, P.M.: The heparin-Ca$^{(2+)}$ interaction: the influence of the O-sulfation pattern on binding. Carbohydr. Res. **339**, 975–983 (2004)
29. Parrish, R.F., Fair, W.R.: Selective binding of zinc ions to heparin rather than to other glycosaminoglycans. Biochem. J. **193**, 407–410 (1981)
30. Zhang, F., Zhang, Z., Lin, X., Beenken, A., Eliseenkova, A.V., Mohammadi, M., Linhardt, R.J.: Compositional analysis of heparin/heparan sulfate interacting with fibroblast growth factor.Fibroblast growth factor receptor complexes. Biochemistry. **48**, 8379–8386 (2009)